High-performance Removal of Anti-inflammatory Using Activated Carbon from Water Treatment Plant Sludge: Fixed-bed and Batch Studies

Alaor Valério Filho
Federal University of Pampa - Bage Campus: Universidade Federal do Pampa
Luana Vaz Tholozan
Federal University of Pampa - Bage Campus: Universidade Federal do Pampa
Aline Lemos Arim
Federal University of Pampa - Bage Campus: Universidade Federal do Pampa
André Ricardo Felkl de Almeida
Federal University of Pampa - Bage Campus: Universidade Federal do Pampa
GABRIELA SILVEIRA DA ROSA (gabrielarosa@unipampa.edu.br)
Universidade Federal do Pampa https://orcid.org/0000-0002-8831-448X

Research Article

Keywords: nimesulide, adsorption, hospital effluent, adsorbent, water treatment plant sludge, factorial design

Posted Date: April 5th, 2021

DOI: https://doi.org/10.21203/rs.3.rs-338372/v1

High-performance removal of anti-inflammatory using activated carbon from water treatment plant sludge: fixed-bed and batch studies

Alaor Valério Filho[a], Luana Vaz Tholozan[b], Aline Lemos Arim[b], André Ricardo Felkl de Almeida[a,b], Gabriela Silveira da Rosa[a,b].

[a.] Graduate Program in Science and Engineering of Materials, Federal University of Pampa, 1650 Maria Anunciação Gomes Godoy Avenue, Bagé, Rio Grande do Sul 96413-172, Brazil.

[b.] Chemical Engineering, Federal University of Pampa, 1650 Maria Anunciação Gomes Godoy Avenue, Bagé, Rio Grande do Sul 96413-172, Brazil

Corresponding author:
Gabriela Silveira da Rosa
email: gabrielarosa@unipampa.edu.br
telephone: +55 53 32473664
fax: +55 53 32473679

Abstract

Activated carbon from water treatment sludge (WASC) was employed as adsorbent material to remove the anti-inflammatory Nimesulide (NM) from aqueous solutions. NM adsorption was performed in batch and fixed-bed systems, evaluating pH, adsorbent dosage, adsorption kinetics, equilibrium isotherm, continuous adsorption, and simulated effluents. The kinetic data were best fitted to the Elovich model and Intraparticle diffusion reaching the equilibrium at 120 min. Langmuir model presented a better description of the equilibrium data with the maximum adsorption capacity (q_{max}) of 274.99 mg g^{-1} from NM adsorption by WASC. The adsorbent was tested in two simulated hospital effluents and proved to be an excellent adsorbent for removing NM from an aqueous solution with the presence of salts, sugars, and other inorganics. Finally, WASC was applied in fixed-bed NM adsorption obtaining the adsorption capacity of 217.28 mg g^{-1}.

Keywords: nimesulide; adsorption; hospital effluent; adsorbent; water treatment plant sludge; factorial design

1 Introduction

The increase of pollutants in the effluents has been considered a major problem for the environment and, consequently, for human life. This situation leads to the reduction of drinking water available (Politano et al. 2017), which is related to global climate change, population growth, industrial and agricultural activity, allied to the improper disposal of contaminants, such as pharmaceuticals in water bodies (Petrie et al. 2015).

Recent researches have indicated the presence of pharmaceutical compounds in effluents and even drinking water, which classify them as emerging contaminants (Sophia A. and Lima 2018). The main origin of contamination of the environment by pharmaceuticals is through domestic and hospital sewages (Seid-Mohammadi et al. 2020), since 30-90% of the ingested is eliminated in urine and feces (Miao et al. 2016). As a consequence of this contamination, the growth of resistant bacteria is causing the inefficiency of usual drugs in the treatment of several diseases (Braschi et al. 2010; Peña-Guzmán et al. 2019).

Regarding emerging pharmaceutical contaminants, the anti-inflammatory NM (nimesulide or 4-nitro-2-phenoxyphenyl) has stood out, due to its wide application in the treatment of pain and inflammations in medicine (Lima et al. 2013), which is a result of its great efficacy compared to similar drugs such as ibuprofen, diclofenac, and piroxicam (Singh et al. 2001). The presence of NM in high concentrations was reported by a study carried out in a sewage treatment plant in Greece (Papageorgiou et al. 2016). Seeking a solution to this problem, studies have investigated the removal of NM from effluents (Gonçalves et al. 2016; Reis et al. 2016; Jauris et al. 2017; Wang et al. 2020).

The adsorption process has been widely applied in the removal of emerging contaminants from effluents due to its several advantages (Streit et al. 2020), such as efficiency, flexibility, low cost, simplicity in application, and low energy consumption (Ahmed 2017; Dotto and McKay 2020). Regarding the adsorption of NM in aqueous solutions, it is worth mentioning Reis et al. (2016), Jauris et al. (2017), Saucier et al. (2015), Pauletto et al. (2020) that used adsorbent materials from sewage sludge, graphene, cocoa shell, and commercial activated carbon, respectively.

The development of alternative adsorbents has been considered a great option for the high cost of conventional adsorbents (Puchana-Rosero et al. 2016; Rovani et al. 2016; Ribeiro et al. 2019; Silva et al. 2020). In this sense, water treatment plant sludge (WTS) has been an excellent raw material (Xu et al. 2015; Valério Filho et al. 2020), as the reuse of this residue is a solution for problems related to the high cost of WTS transport, which causes it to be discarded, frequently, in nearby water bodies (Dassanayake et al. 2015; Hidalgo et al. 2017). Moreover, the WTS has important characteristics such as alumina and silica in its composition that can assist in the formation of functional surface groups that have a good interaction with various contaminants present in effluents (Siswoyo et al. 2019).

Thus, the objective of this work was to apply activated carbon from water treatment plant sludge in the adsorption of anti-inflammatory NM. The batch analysis was done by evaluating initial pH, adsorbent dosage, adsorption kinetics, and isotherm. The study also emphasized the treatment of simulated hospital wastewater and the fixed-bed adsorption of NM by WASC, as a proposal for industrial application.

2 Materials and Methods

2.1 Materials and solutions

NM, with purity ≥98%, and all other reagents (analytical grade) were purchased from Sigma-Aldrich, Brazil. NM was used in this study without further purification. To improve the NM solubilization, the solution was prepared with a solution of ethanol (20% v/v).

2.2 Production and characterization of activated carbon

WTS was collected at the water treatment plant in the city of Bagé, Brazil (31°18'22.5"S 54°07'20.0"W). The sample was activated with $ZnCl_2$ and $CaOH_2$ and then pyrolysis was performed at 550ºC for 30 min. Then acid leaching with HCl was applied to remove remaining inorganics. The activated carbon produced was named washed activated sludge carbon (WASC) and was characterized using BET, FTIR, DRX, and TGA techniques, the details can be found in a previous paper (Valério Filho et al.).

The reactive groups present on the surface of WASC before and after the NM adsorption were obtained by the Fourier Transform Infrared Spectroscopy (Shimadzu IR Prestige-21, Japan) technique. The spectrum was performed in the range of 500-4500 cm^{-1} with a resolution of 4 cm^{-1}.

2.3 Batch studies

NM solution of 25 mL (15-800 mg L^{-1}) was added in contact with WASC (0.4-1.6 g L^{-1}). The pH value was investigated in the range of 8 to 11 (adjusted with NaOH). A shaker (NOVA ÉTICA, 109-1, Brazil) was used to agitate the mixtures, between 5 and 240 min, at 150 rpm. The samples were centrifuged (QUÍMIS, Q222TM216, Brazil) to separate the activated carbon from the NM solution. The concentration of NM was evaluated using standard known concentrations, at the maximum wavelength of 392 nm, in a UV-VIS spectrophotometer (Kazuaki, II-226, China). Equations 1 and 2 were used to determine the adsorption capacity, (q_e, mg g^{-1}) and removal efficiency (E, %), respectively.

$$q_e = \frac{(C_i - C_e)V}{m} \quad (1)$$

$$E = \frac{C_i - C_e}{C_i} \quad (2)$$

where C_i is the initial NM concentration (mg L^{-1}); C_e, equilibrium NM concentration (mg L^{-1}); M, the mass of WASC (g); and V, the volume of solution (L).

2.4 Statistical analysis

2^2 Factorial Design (FD) was applied at a 95% confidence level to understand which factor (adsorbent dosage (A_d (g L^{-1})) and initial pH) would have a major impact on adsorption processes and how these parameters would interact between them. This method was also used to develop a mathematical model to describe the adsorption process. Table 1 shows the independent variables and respective levels used in the experimental design.

Table 1 Independent variables and levels of experimental design.

The FD was carried out with independent variables at 3 levels and it was arbitrated 3 repetitions of the central point to provide an estimate of pure error.

2.5 Kinetic and isotherm studies

Four kinetic models were tested to describe experimental data: the pseudo-first order, pseudo-second order, intraparticle diffusion, and Elovich kinetic models were adjusted to experimental data. These models are represented by Equations 3-6, respectively.

$$q_t = q_e(1 - e^{-k_1 t}) \quad (3)$$

$$q_t = \frac{q_e{}^2(k_2 t)}{(1 + q_e k_2 t)} \quad (4)$$

$$q_t = k_{int} t^{1/2} + C \quad (5)$$

$$q_e = \frac{1}{\alpha}\ln(1 + \alpha\beta t) \quad (6)$$

where t is the time of contact (min); q_t is the amount of NM adsorbed at time t (mg g^{-1}); k_1 is the pseudo-first order rate constant (min^{-1}); k_2 is the pseudo-second order rate constant (g mg^{-1} min^{-1}); k_{id} is the rate constant for intraparticle diffusion (g mg^{-1} $min^{-1/2}$); C is related to diffusion resistance (mg g^{-1}); α is the initial rate of Elovich model (mg g^{-1} min^{-1}); and β is the Elovich model constants (mg g^{-1}).

Langmuir and Freundlich isotherm models were applied to analyze the equilibrium experimental data. These models are represented in Equations 7 and 8, respectively.

$$q_e = \frac{q_{max} K_L C_e}{1 + K_L C_e} \quad (7)$$

$$q_e = K_F C_e^{\frac{1}{n_F}} \quad (8)$$

where q_{max} is the maximum adsorption capacity of the adsorbent (mg g^{-1}), k_L is the Langmuir equilibrium constant (L mg^{-1}); k_F is the Freundlich equilibrium constant ($mg^{1-(1/n)}$ $L^{1/n}$ /g) and $1/n_F$ is the Freundlich exponent.

All model parameters were defined by nonlinear regression, using the quasi-Newton method. The adequacy of the models was analyzed by variance analysis (ANOVA) checked by $F_{value} > F_{tabled}$, were F_{value} is the regression coefficient. Furthermore, the models were checked by using the Chi-square (X^2) and average relative error (ARE) according to Equations 9 and 10, respectively.

$$ARE = \frac{100}{nn}\sum \frac{q_{exp} - q_{pred}}{q_{exp}} \quad (9)$$

$$X^2 = \sum \frac{(q_{exp} - q_{pred})^2}{nn - NN} \quad (10)$$

where q_{exp} are the experimental values; q_{pred} is the value of the model, nn is the experiment number observed, and NN is the number of the parameters in the model.

2.6 Simulated hospital wastewater

In this study, two simulated hospital effluents were produced to evaluate NM adsorption by WASC in the middle of sugars, high salt, urea, and other inorganics commonly found in hospital waste effluents (Saucier et al. 2015). Table 2 shows the composition of the simulated effluents.

Table 2 Chemical composition of simulated hospital effluents.

2.7 Continuous adsorption studies

The fixed-bed tests were performed on glass columns using 1 g of WASC. Two columns were used, the internal diameter of column 1 is 5 mm and the bed height 50.4 mm, column 2 has an internal

diameter of 9 mm and 28 mm of bed height. The NM solution (200 mg L^{-1}) was used to feed the bed with a flow rate of 10 mL min^{-1}. Thomas and Yoon-Nelson models were fitted to the experimental fixed-bed data for an estimate of the kinetic parameters, they are represented in Equations 11 and 12, respectively.

$$C_t = \frac{C_e}{1+\exp(\frac{K_{th}\, q_{th}\, m}{Q} - k_{th}\, C_e t)} \quad (11)$$

$$C_t = \frac{C_e}{1 + \exp(k_{yn}\,(\tau_h - t))} \quad (12)$$

were k_{th} is the Thomas rate constant (mL mg^{-1} min^{-1}); q_{max} is the maximum adsorption capacity of Thomas model (mg g^{-1}); Q is the flow rate (mL min^{-1}); k_{yn} is the Yoon-Nelson rate constant (min^{-1}); and τ_h is the time required for 50% solute breakthrough (min).

3 Results and Discussion

Table 3 presents the experimental design of the interaction between adsorbent dosage (A_d) and pH, and the results of adsorption capacity and efficiency of removal of NM by WASC.

Table 3. Experimental results for capacity and efficiency of NM adsorption. Conditions: C_i, 30 mg L^{-1}; contact time, 60 min; temperature, room temperature (25 ± 2ºC).

The low standard deviation results (0.03-0.91 mg g^{-1} and 0.10-1.96%) indicate the reproducibility of the experiments. The highest value of q_e was 45.06 mg g^{-1} (run 1), which corresponds to an efficiency of 59.77%, and the highest value for E was 95.31%, which corresponds to an adsorption capacity of 17.83 mg g^{-1}.

Fig. 1 presents the estimated effects in the adsorption process of NM by WASC for adsorption capacity and efficiency. The reverse elimination process was applied in the statistical analysis of the model, excluding non-significant dependent terms (da Rosa et al. 2019).

Fig. 1 Pareto charts of the estimated effects on adsorption capacity (a) and efficiency (b)

Analyzing the results plotted in pareto charts it can be inferred that the pH is the most significant effect on the adsorption capacity and efficiency of NM. Fig. 1(a) indicates that all parameters were significant for adsorption capacity ($p>0.05$). The pH was the parameter with the most pronounced negative effect. There is a linear dependence between the pH and the adsorbent performance, this is, the adsorption capacity decreases with the increase of pH. The interaction between A_d and pH had a positive effect and A_d had a negative effect.

From the adsorption efficiency presenting in Fig. 1(b), the more pronounced effect was the pH with the negative effect. The A_d parameters had a positive effect and the interaction between A_d and pH was not significant ($p \leq 0.05$). The A_d antagonist behavior from adsorption capacity and efficiency can be explained by the high values of A_d, which promotes an increase in adsorption efficiency. Although it increases the presence of free sites in WASC and, consequently, leads to the decreasing of adsorption capacity. Due to this, the central point 1 g L^{-1} for A_d was chosen to continue the batch tests.

The pH of the solution is an important factor to be observed during pharmaceutical adsorption because affects the surface charge of the adsorbent (Arim et al. 2018). Studies have already reported that in solutions at pH lower than 7 the NM precipitates (Saucier et al. 2015; Jauris et al. 2017). Fig. 1(a-b) and Table 3 indicates that the best pH condition for a higher q_e was at initial pH 8. The higher the pH, the lower the concentration of H^+ ions. This indicates that the WASC surface must be negative and that interaction between WASC-NM does not occur electrostatically (Saucier et al. 2015). The interaction probably occurs through H bonding and van der Waals forces (Saucier et al. 2015; Jauris et al. 2017).

The kinetic behavior of NM adsorption by WASC and the adjustments of the pseudo-first order, pseudo-second order, Elovich, and intraparticle diffusion mathematical models are presented in Fig. 2**.**

Fig. 2 Kinetic curves and mathematical model adjustments of pseudo-first order, pseudo-second order, and Elovich models (a) and intraparticle diffusion (b). Conditions: C_i, 30 mg L^{-1}; pH, 8;A_d, 1 g L^{-1}; temperature, room temperature (25 ± 2ºC).

It can be observed in Fig. 2(a) that the sorption rate is higher at the beginning of the process because of the greater number of active sites on the surface of the adsorbent (Arim et al. 2019). The experimental data show that most NM was removed around 90 minutes and no significant changes in terms of removal were observed after 120 min.

Fig. 2(b) presenting the limiting rate step for the adsorption process of NM onto WASC, using the intraparticle diffusion model. Three steps can be identified in the kinetic plots. The first step is related to the surface diffusion, with the mass transfer of the NM to the external surface of the WASC particles (Alves et al. 2013). The second step is related to the intraparticle diffusion and the third step indicates the equilibrium phase due to the NM occupation of all the active sites of WASC (Arim et al. 2018).

The kinetic parameter values obtained from the fitting of the kinetic models to experimental data are presented in Table 4.

Table 4 Kinetic parameters of NM anti-inflammatory adsorption in WASC.

All models were checked by the statistical significance through the regression F test and the values obtained indicated which models presented a good fit. The Elovich and Intraparticle diffusion models describe better the adsorption kinetic as indicated by the highest coefficient of determination, R^2, even though the Intraparticle diffusion model shows the lowest values for X^2 and ARE. The parameters values of intraparticle diffusion obtained from NM adsorption onto WASC were k_{int}= 1.94 g mg^{-1} $min^{-1/2}$ and C= 7.93 mg g^{-1} which represents intraparticle rate constants and boundary layer thickness, respectively (Al-Rashdi et al. 2012; Arim et al. 2018). The C values different from zero indicate that more mechanisms were involved in NM adsorption (Arim et al. 2018).

The good fit for the Elovich model can indicate the presence of chemisorption in NM removal, not a first-order reaction [30], such behavior is confirmed to the high adjustment for the pseudo-second order model. This means that the NM molecule was dissociated into independent fragments creating radicals and atoms attached to the adsorbent (Dotto and McKay 2020). The parameters α (0.2142 mg g^{-1} min^{-1}) and β

(9.89 mg g^{-1}) of this model represent the initial rate of chemisorption and the number of sites available for NM adsorption, respectively. The Pseudo-first order model has also presented a good fit, which indicates that van der Waals forces and H bonding can occur in the NM adsorption (Saucier et al. 2015; Jauris et al. 2017).

The equilibrium experimental data of NM adsorption onto WASC and the adjustment of the isotherm models are presented in Fig. 3 and their parameters in Table 5**.**

Fig. 3 Isotherm curve from adsorption of NM on WASC. Conditions: C_i, 15-800 mg L^{-1}; pH, 8; A_d, 1 g L^{-1}; contact time, 180 min; temperature, room temperature (25 ± 2ºC).

Table 5. Isotherm parameters of NM anti-inflammatory adsorption in WASC

The isotherm curves (Fig. 3) indicate a favorable adsorption process from NM adsorption onto WASC, it occurs when the increase of the adsorption capacity and the increase of adsorbate concentration are proportional (Silva et al. 2020). The good results for NM adsorption can be related to the WASC surface area of 582.0 m^2 g^{-1}. Also, the predominant mesoporous size distribution (3.02 nm) for WASC (Valério Filho et al.) and the extreme distances between the atoms of NM molecule of 0.993 nm (Saucier et al. 2015) indicate that WASC is capable to adsorb NM anti-inflammatory.

The Langmuir isotherm is the best model for describing the experimental data, considering the highest values of R^2 and F_{value} and also the lowest values of X^2 and ARE. The maximum sorption capacity of NM onto WASC was 274.99 mg g^{-1}, the value is superior to studies that have already investigated the adsorption of NM. The maximum sorption of NM previously reported in the literature was q_{max} of 14.18 mg.g^{-1}, using a silica aerogel (Caputo et al. 2012); q_{max} of 26.12 mg.g^{-1}, using a combination of polysiloxanes and sewage sludge (Simões dos Reis et al. 2016); q_{max} of 66.45 mg.g^{-1}, using activated carbon from sewage sludge (Reis et al. 2016); q_{max} of 74.81 mg.g^{-1}, using activated carbon from cocoa shell (Saucier et al. 2015); and q_{max} of 82.4 mg.g^{-1}, using a graphene material (Jauris et al. 2017). Due to the excellent values for maximum adsorption capacity, in Fig. 4 the adsorption of NM by WASC was analyzed in a competitive environment with other inorganics, sugars, and salts. The chemical composition of simulated hospital effluents is showing in Table 2.

Fig. 4 Adsorption efficiency of NM in hospital effluents treatment with WASC. Conditions: pH, 8; A_d, 1 g L^{-1}; contact time, 180 min; temperature, room temperature (25 ± 2ºC).

The application of the adsorbent material in simulated effluent provides important information regarding the efficiency of this adsorbent in competitive effluents (Wamba et al. 2019). The WASC impressively adsorbed 98.57 % and 88.08 % of NM in the hospital effluent A and B, respectively. Using activated carbon from cocoa shell, Saucier (Saucier et al. 2015) reported efficiency of 95.58 % in the removal of NM from simulated hospital effluent using an adsorbent dosage of 2.5 g L^{-1}. This result indicates that WASC was a great and sustainable option for the utilization of WTS as an adsorbent for NM removal from hospital wastewater.

Fig. 5 shows the continuous adsorption of NM by WASC. The influence of bed height and length was analyzed in two beds with different diameters and fixed adsorbent mass and flow rate.

Fig. 5. Fixed-bed adsorption of NM onto WASC. Conditions: C_i, 200 mg L^{-1}; pH, 8; WASC mass, 1 g; temperature, room temperature (25 ± 2ºC); flow rate, 10 ml min^{-1}.

Fig. 5 showed that the small internal diameters and, consequently, higher bed height provide better conditions from the NM adsorption by the WASC. This is related to the interaction time between NM-WASC in the column. The 52 mm bed height provides a longer interaction time than the 28 mm height. Such occurrence is in agreement with the kinetic curves presented in Fig. 2, where it was observed that the adsorption of NM does not occur in an instantaneous way, such behavior in fixed-bed confirms that the adsorption of NM is mainly controlled by chemisorption (Patel 2020). This means that greater bed heights will allow for better performance because the unused fraction of WASC is reduced. WASC saturation time was longer for column 1 than for column 2, this is also related to the greater use of the adsorbent bed and consequently greater adsorption capacity.

To describe the dynamic behavior of the column, the Thomas and Yoon-Nelson models (Equations 11 and 12) were fitted to the experimental data. Table 6 summarizes the parameters found for each model and the respective error parameters (R^2, $X^{2,}$ and *ARE*).

Table 6 Model parameters of the fixed-bed NM adsorption onto WASC

Thomas and Yoon-Nelson models showed a good fit for both columns with high values for R^2. Column 1 presents higher values from R^2 and lower values from X^2 and *ARE* in comparison with Column 2. The explanation for this is that the adjustments can better predict the fixed bed curve when the adsorbent is saturated by NM molecules (Dotto and McKay 2020). The saturation of 1 g of WASC occurs for column 1 obtaining q_{max} of 217.28 mg g^{-1}.

Fig. 6 shows the intensity of the molecular groups present in WASC before and after the NM adsorption.

Fig. 6. FT-IR spectra for WASC before and after the NM adsorption

After the adsorption, WASC demonstrates a decrease in alcoholic and phenolic O-H groups (a) compared to before the NM adsorption, it is represented by the intense band between 3600-3400 cm^{-1} (Calvete et al. 2010a, b; da Silva et al. 2011). The band range at 1700-1400 cm^{-1} indicates the presence of C=O carboxylic acid stretching in WASC (b), the interference can be related to NH bend of NM (Caputo et al. 2012; Saucier et al. 2015). The 940-665 cm^{-1} band in WASC before the adsorption, indicates the presence of bending O-H (c) (Puchana-Rosero et al. 2016). The decrease in the O-H groups may be related to the disruption of these groups due to the interaction with NM molecules through H bonding (Saucier et al. 2015; Jauris et al. 2017).

Based on the results of this work, it is possible to infer that the NM-WASC interaction is mainly controlled by intraparticle diffusion and chemisorption, but also presents attraction forces of H bonding. This great interaction of adsorbent-adsorbate might have positively influenced the high values obtained from q_{max} of isotherm studies and fixed-bed adsorption.

4. Conclusion

The WASC showed excellent results for the removal of NM anti-inflammatory. FD was successful in predicting the optimal pH 8 and A_d values. The equilibration time was reached in 120 min and the models that better described the kinetics data were the Intraparticle diffusion and Elovich model. The maximum amount adsorbed (q_{max}) of NM in batch tests was 274.99 mg g^{-1} and the isotherm data were better described by the Langmuir model. WASC proved to be efficient in the treatment of hospital wastewater, obtaining an impressive adsorption efficiency of 98.57% in a competitive environment with sugars, salts, and other inorganics. Finally, WASC was used in a fixed-bed for adsorption of NM in a continuous system, obtaining q_{max} values of 217.28 mg g^{-1}, saturating in 250 min at a flow rate of 10 mL min^{-1}. The results obtained in this work prove that WASC is an extremely promising adsorbent in the treatment of real pharmaceutical effluents.

Data availability

Not applicable.

Consent for publication

Not applicable.

Availability of data and materials

All data generated or analyzed during this study are included in this published article and its supplementary information files.

Competing interests

The authors declare that they have no competing interests.

Funding

Not applicable

Acknowledgements

The authors would like to thank the Federal University of Pampa (UNIPAMPA) for having made available its laboratory structure to carry out this work.

Ethics approval and consent to participate

Not applicable.

Authors contributions

Alaor Valério Filho: Conceptualization, methodology, investigation, formal analysis, visualization, and writing

Luana Vaz Tholozan: Writing and editing

Aline Lemos Arim: Investigation and paper review

André R. F. de Almeida: Formal analysis, methodology, and paper review

Gabriela S. da Rosa: Conceptualization, methodology, investigation, and writing of the review and editing.

339

340 **References**

341 Ahmed MJ (2017) Adsorption of non-steroidal anti-inflammatory drugs from aqueous solution using
342 activated carbons: Review. J Environ Manage 190:274–282.
343 https://doi.org/10.1016/j.jenvman.2016.12.073

344 Al-Rashdi B, Tizaoui C, Hilal N (2012) Copper removal from aqueous solutions using nano-scale diboron
345 trioxide/titanium dioxide (B2O3/TiO2) adsorbent. Chem Eng J 183:294–302.
346 https://doi.org/10.1016/j.cej.2011.12.082

347 Alves CCO, Franca AS, Oliveira LS (2013) Removal of phenylalanine from aqueous solutions with
348 thermo-chemically modified corn cobs as adsorbents. LWT - Food Sci Technol 51:1–8.
349 https://doi.org/10.1016/j.lwt.2012.11.012

350 Arim AL, Quina MJ, Gando-Ferreira LM (2019) Uptake of trivalent chromium from aqueous solutions by
351 xanthate pine bark: Characterization, batch and column studies. Process Saf Environ Prot 121:374–
352 386. https://doi.org/10.1016/j.psep.2018.11.001

353 Arim AL, Quina MJ, Gando-Ferreira LM (2018) Insights into the Sorption Mechanisms of Cr(III) by
354 Chemically Modified Pine Bark. Chem Eng Technol 41:1378–1389.
355 https://doi.org/10.1002/ceat.201800034

356 Braschi I, Blasioli S, Gigli L, et al (2010) Removal of sulfonamide antibiotics from water: Evidence of
357 adsorption into an organophilic zeolite Y by its structural modifications. J Hazard Mater 178:218–
358 225. https://doi.org/10.1016/j.jhazmat.2010.01.066

359 Calvete T, Lima EC, Cardoso NF, et al (2010a) Application of carbon adsorbents prepared from
360 Brazilian-pine fruit shell for the removal of reactive orange 16 from aqueous solution: Kinetic,
361 equilibrium, and thermodynamic studies. J Environ Manage 91:1695–1706.
362 https://doi.org/10.1016/j.jenvman.2010.03.013

363 Calvete T, Lima EC, Cardoso NF, et al (2010b) Removal of brilliant green dye from aqueous solutions
364 using home made activated carbons. Clean - Soil, Air, Water 38:521–532.
365 https://doi.org/10.1002/clen.201000027

366 Caputo G, Scognamiglio M, De Marco I (2012) Nimesulide adsorbed on silica aerogel using supercritical
367 carbon dioxide. Chem Eng Res Des 90:1082–1089. https://doi.org/10.1016/j.cherd.2011.11.011

368 da Rosa GS, Vanga SK, Gariepy Y, Raghavan V (2019) Comparison of microwave, ultrasonic and
369 conventional techniques for extraction of bioactive compounds from olive leaves (Olea europaea
370 L.). Innov Food Sci Emerg Technol 58:102234. https://doi.org/10.1016/j.ifset.2019.102234

371 da Silva LG, Ruggiero R, Gontijo P de M, et al (2011) Adsorption of Brilliant Red 2BE dye from water
372 solutions by a chemically modified sugarcane bagasse lignin. Chem Eng J 168:620–628.
373 https://doi.org/10.1016/j.cej.2011.01.040

374 Dassanayake KB, Jayasinghe GY, Surapaneni A, Hetherington C (2015) A review on alum sludge reuse
375 with special reference to agricultural applications and future challenges. Waste Manag 38:321–335.
376 https://doi.org/10.1016/j.wasman.2014.11.025

377 Dotto GL, McKay G (2020) Current scenario and challenges in adsorption for water treatment. J Environ
378 Chem Eng 8:103988. https://doi.org/10.1016/j.jece.2020.103988

379 Gonçalves AA, Araújo AF, De Mesquita JP, et al (2016) Characterisation of silica-supported Fe-Ni
380 bimetallic nanoparticles and kinetic study of reductive degradation of the drug nimesulide. J
381 Environ Chem Eng 4:4354–4365. https://doi.org/10.1016/j.jece.2016.09.038

382 Hidalgo AM, Murcia MD, Gómez M, et al (2017) Possible Uses for Sludge from Drinking Water
383 Treatment Plants. J Environ Eng (United States) 143:1–7. https://doi.org/10.1061/(ASCE)EE.1943-
384 7870.0001176

385 Jauris IM, Matos CF, Zarbin AJG, et al (2017) Adsorption of anti-inflammatory nimesulide by graphene
386 materials: A combined theoretical and experimental study. Phys Chem Chem Phys 19:22099–
387 22110. https://doi.org/10.1039/c7cp04272h

388 Lima AB, Chaves SC, Silva LM da, et al (2013) Determinação de nimesulida por análise por injeção em
389 fluxo com detecção amperométrica de múltiplos pulsos. Quim Nova 36:1296–1302.
390 https://doi.org/10.1590/S0100-40422013000900004

391 Miao MS, Liu Q, Shu L, et al (2016) Removal of cephalexin from effluent by activated carbon prepared
392 from alligator weed: Kinetics, isotherms, and thermodynamic analyses. Process Saf. Environ. Prot.
393 104:481–489

394 Papageorgiou M, Kosma C, Lambropoulou D (2016) Seasonal occurrence, removal, mass loading and
395 environmental risk assessment of 55 pharmaceuticals and personal care products in a municipal
396 wastewater treatment plant in Central Greece. Sci Total Environ 543:547–569.
397 https://doi.org/10.1016/j.scitotenv.2015.11.047

398 Patel H (2020) Batch and continuous fixed bed adsorption of heavy metals removal using activated
399 charcoal from neem (Azadirachta indica) leaf powder. Sci Rep 10:1–12.
400 https://doi.org/10.1038/s41598-020-72583-6

401 Pauletto PS, Lütke SF, Dotto GL, Salau NPG (2020) Forecasting the multicomponent adsorption of
402 nimesulide and paracetamol through artificial neural network. Chem Eng J 127527.
403 https://doi.org/10.1016/j.cej.2020.127527

404 Peña-Guzmán C, Ulloa-Sánchez S, Mora K, et al (2019) Emerging pollutants in the urban water cycle in
405 Latin America: A review of the current literature. J Environ Manage 237:408–423.
406 https://doi.org/10.1016/j.jenvman.2019.02.100

407 Petrie B, Barden R, Kasprzyk-Hordern B (2015) A review on emerging contaminants in wastewaters and
408 the environment: Current knowledge, understudied areas and recommendations for future

409 monitoring. Water Res 72:3–27. https://doi.org/10.1016/j.watres.2014.08.053

410 Politano A, Argurio P, Di Profio G, et al (2017) Photothermal Membrane Distillation for Seawater
411 Desalination. Adv Mater 29:1–6. https://doi.org/10.1002/adma.201603504

412 Puchana-Rosero MJ, Adebayo MA, Lima EC, et al (2016) Microwave-assisted activated carbon obtained
413 from the sludge of tannery-treatment effluent plant for removal of leather dyes. Colloids Surfaces A
414 Physicochem. Eng. Asp. 504:105–115

415 Reis GS dos, Bin Mahbub MK, Wilhelm M, et al (2016) Activated carbon from sewage sludge for
416 removal of sodium diclofenac and nimesulide from aqueous solutions. Korean J Chem Eng
417 33:3149–3161. https://doi.org/10.1007/s11814-016-0194-3

418 Ribeiro PB, de Freitas VO, Machry K, et al (2019) Evaluation of the potential of coal fly ash produced by
419 gasification as hexavalent chromium adsorbent. Environ Sci Pollut Res 26:28603–28613.
420 https://doi.org/10.1007/s11356-018-3852-7

421 Rovani S, Rodrigues AG, Medeiros LF, et al (2016) Synthesis and characterisation of activated carbon
422 from agroindustrial waste - Preliminary study of 17β-estradiol removal from aqueous solution. J
423 Environ Chem Eng 4:2128–2137. https://doi.org/10.1016/j.jece.2016.03.030

424 Saucier C, Adebayo MA, Lima EC, et al (2015) Microwave-assisted activated carbon from cocoa shell as
425 adsorbent for removal of sodium diclofenac and nimesulide from aqueous effluents. J Hazard Mater
426 289:18–27. https://doi.org/10.1016/j.jhazmat.2015.02.026

427 Seid-Mohammadi A, Asgarai G, Ghorbanian Z, Dargahi A (2020) The removal of cephalexin antibiotic in
428 aqueous solutions by ultrasonic waves/hydrogen peroxide/nickel oxide nanoparticles
429 (US/H2O2/NiO) hybrid process. Sep Sci Technol 55:1558–1568.
430 https://doi.org/10.1080/01496395.2019.1603241

431 Silva EO da, dos Santos VD, de Araujo EB, et al (2020) Removal of methylene blue from aqueous
432 solution by ryegrass straw. Int J Environ Sci Technol 17:3723–3740.
433 https://doi.org/10.1007/s13762-020-02718-9

434 Simões dos Reis G, Sampaio CH, Lima EC, Wilhelm M (2016) Preparation of novel adsorbents based on
435 combinations of polysiloxanes and sewage sludge to remove pharmaceuticals from aqueous
436 solutions. Colloids Surfaces A Physicochem Eng Asp 497:304–315.
437 https://doi.org/10.1016/j.colsurfa.2016.03.021

438 Singh A, Singh P, Kapoor VK (2001) Nimesulide. Anal Profiles Drug Subst Excipients 28:197–249.
439 https://doi.org/10.1016/S1075-6280(01)28006-9

440 Siswoyo E, Qoniah I, Lestari P, et al (2019) Development of a floating adsorbent for cadmium derived
441 from modified drinking water treatment plant sludge. Environ Technol Innov 14:100312.
442 https://doi.org/10.1016/j.eti.2019.01.006

443 Sophia A. C, Lima EC (2018) Removal of emerging contaminants from the environment by adsorption.

444 Ecotoxicol Environ Saf 150:1–17. https://doi.org/10.1016/j.ecoenv.2017.12.026

445 Streit AFM, Collazzo GC, Druzian SP, et al (2020) Adsorption of ibuprofen, ketoprofen, and paracetamol
446 onto activated carbon prepared from effluent treatment plant sludge of the beverage industry.
447 Chemosphere. https://doi.org/10.1016/j.chemosphere.2020.128322

448 Valério Filho A, Kulman RX, Janner NN, et al Optimization of cationic dye removal using a high surface
449 area-activated carbon from water treatment sludge. Bull Mater Sci. https://doi.org/10.1007/s12034-
450 020-02333-x

451 Valério Filho A, Xavaré Kulman R, Tholozan LV, et al (2020) Preparation and Characterization of
452 Activated Carbon Obtained from Water Treatment Plant Sludge for Removal of Cationic Dye from
453 Wastewater. Processes 8:1549. https://doi.org/10.3390/pr8121549

454 Wamba AGN, Ndi SK, Lima EC, et al (2019) Preparation, characterization of titanate nanosheet–
455 pozzolan nanocomposite and its use as an adsorbent for removal of diclofenac from simulated
456 hospital effluents. J Taiwan Inst Chem Eng 102:321–329.
457 https://doi.org/10.1016/j.jtice.2019.05.001

458 Wang Z, Nengzi L chao, Zhang X, et al (2020) Novel NiCo2S4/CS membranes as efficient catalysts for
459 activating persulfate and its high activity for degradation of nimesulide. Chem Eng J 381:122517.
460 https://doi.org/10.1016/j.cej.2019.122517

461 Xu G, Yang X, Spinosa L (2015) Development of sludge-based adsorbents: Preparation, characterization,
462 utilization and its feasibility assessment. J Environ Manage 151:221–232.
463 https://doi.org/10.1016/j.jenvman.2014.08.001

464

Figures

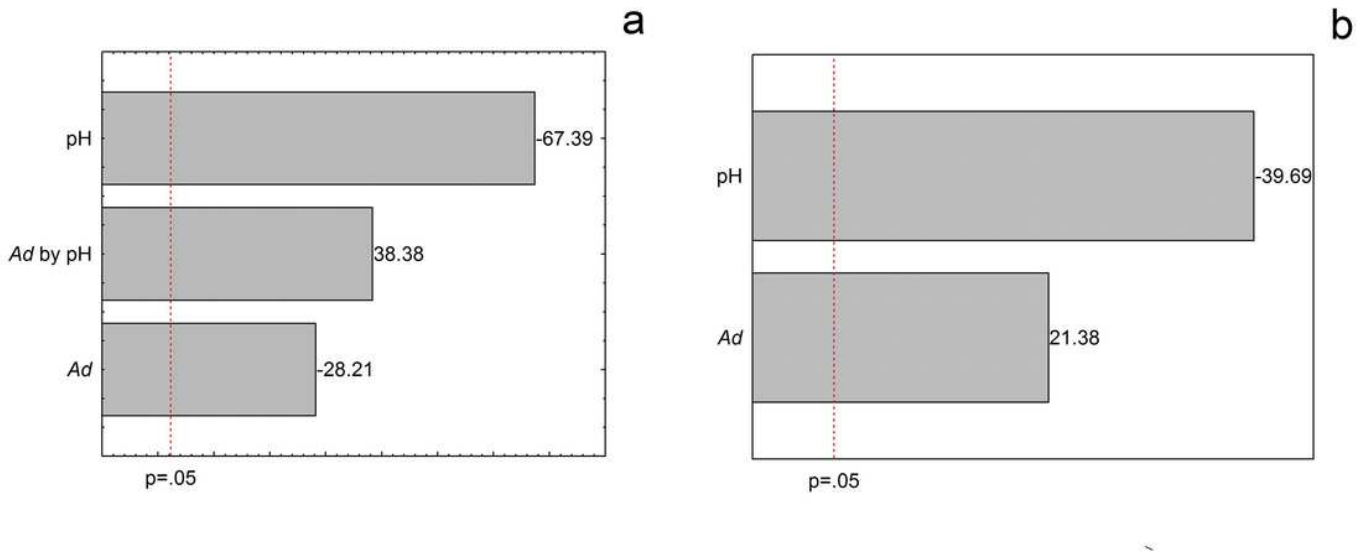

Figure 1

Pareto charts of the estimated effects on adsorption capacity (a) and efficiency (b)

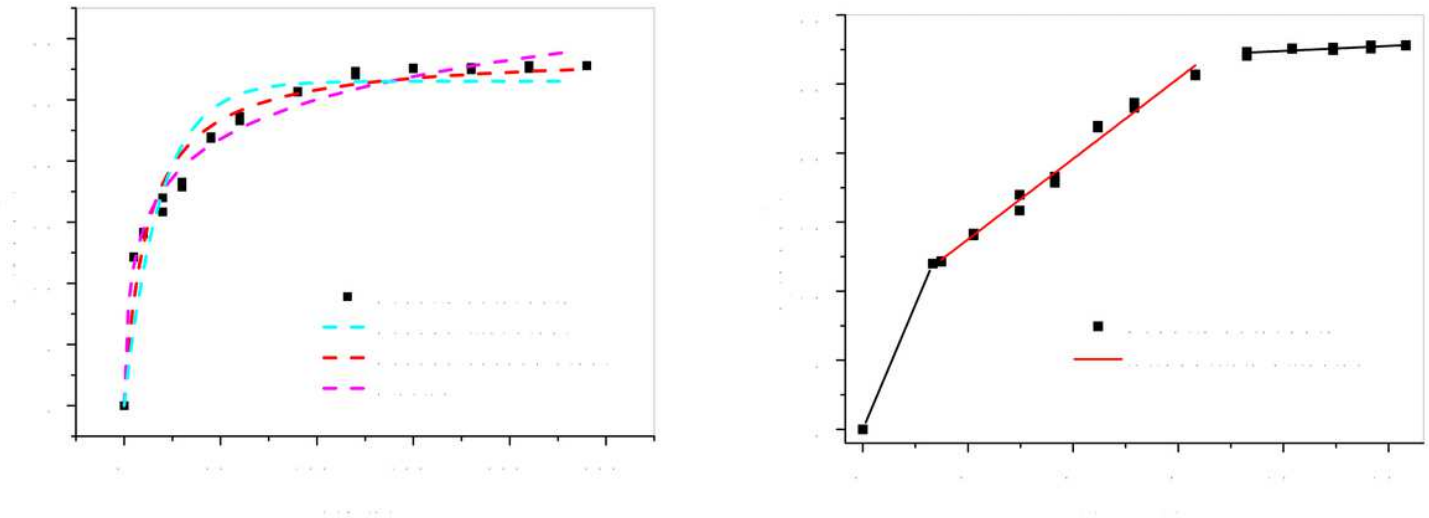

Figure 2

Please see the Manuscript PDF file for the complete figure caption

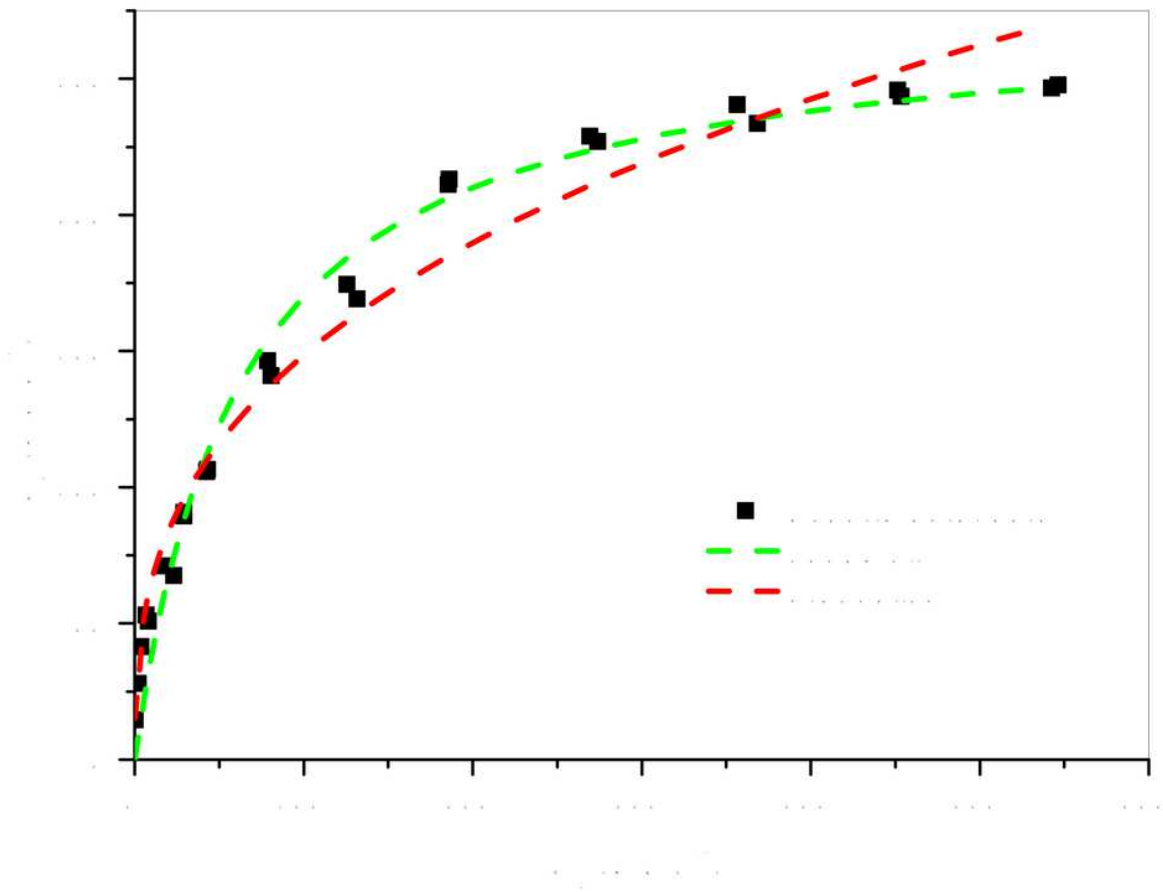

Figure 3

Please see the Manuscript PDF file for the complete figure caption

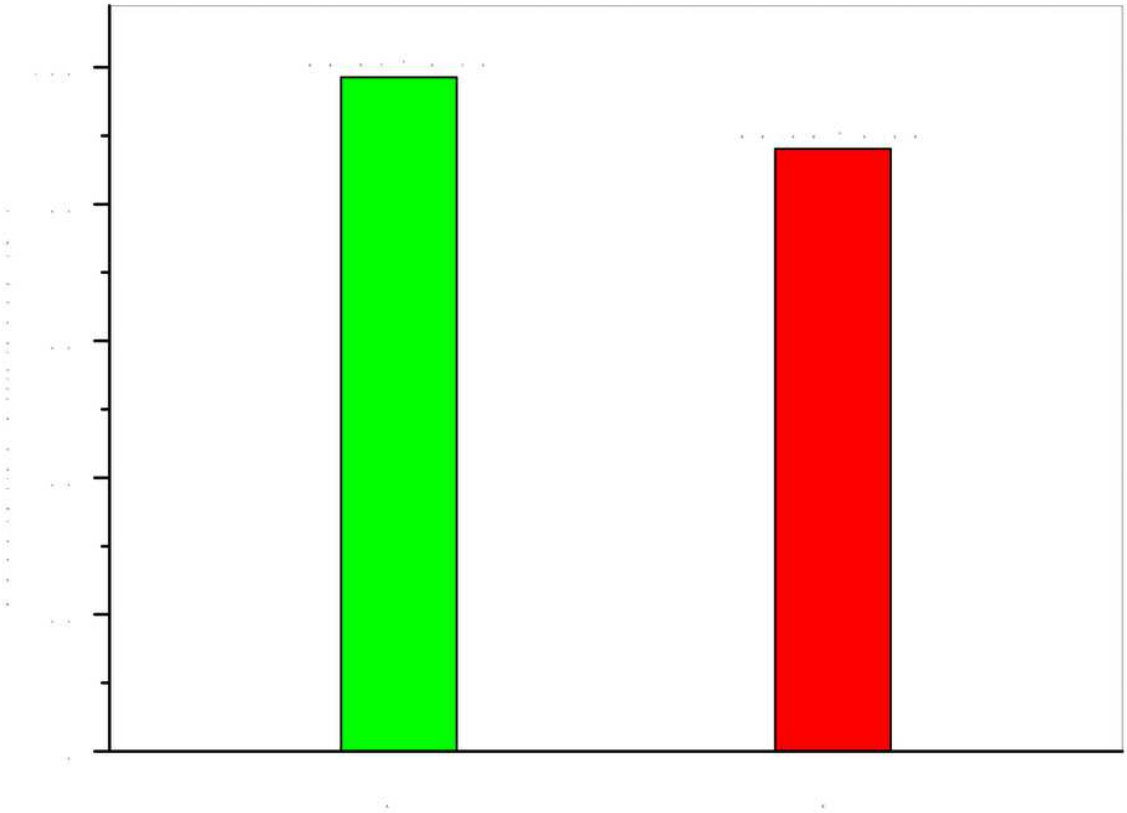

Figure 4

Please see the Manuscript PDF file for the complete figure caption

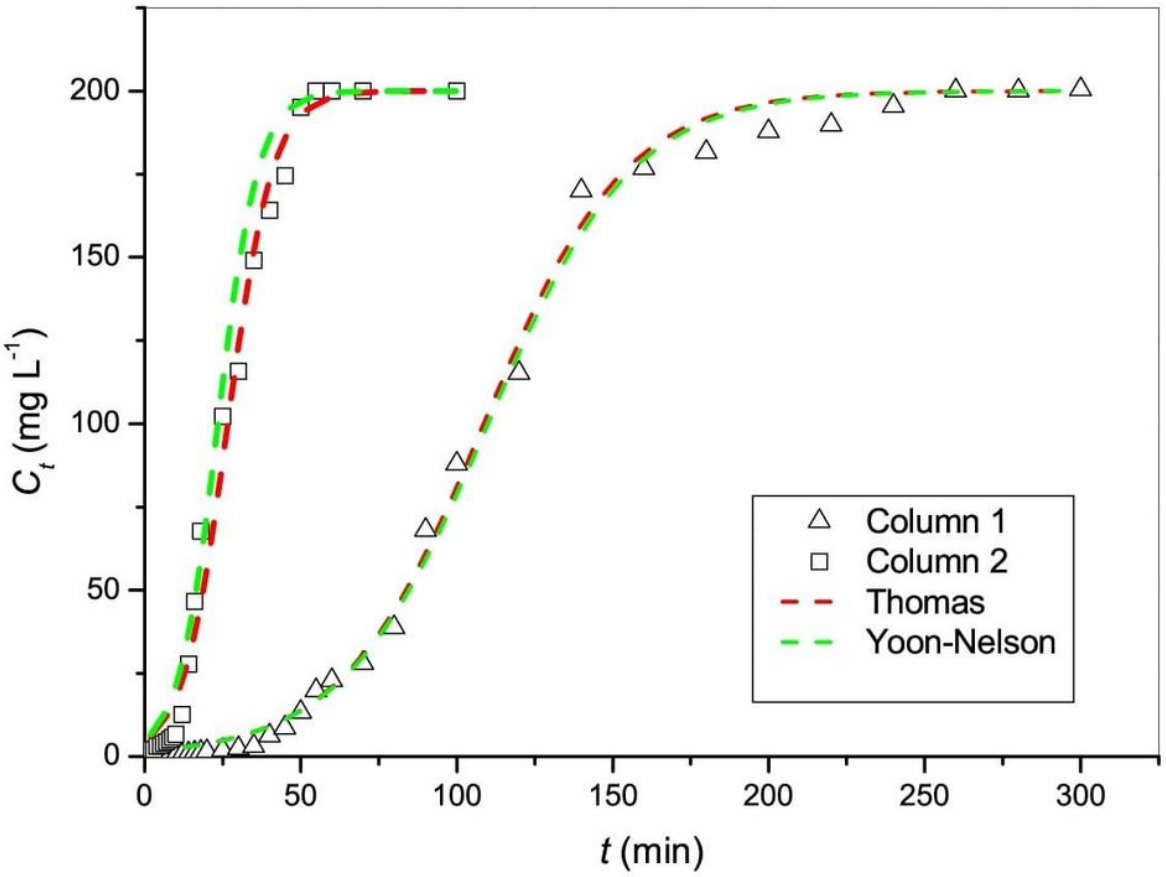

Figure 5

Please see the Manuscript PDF file for the complete figure caption

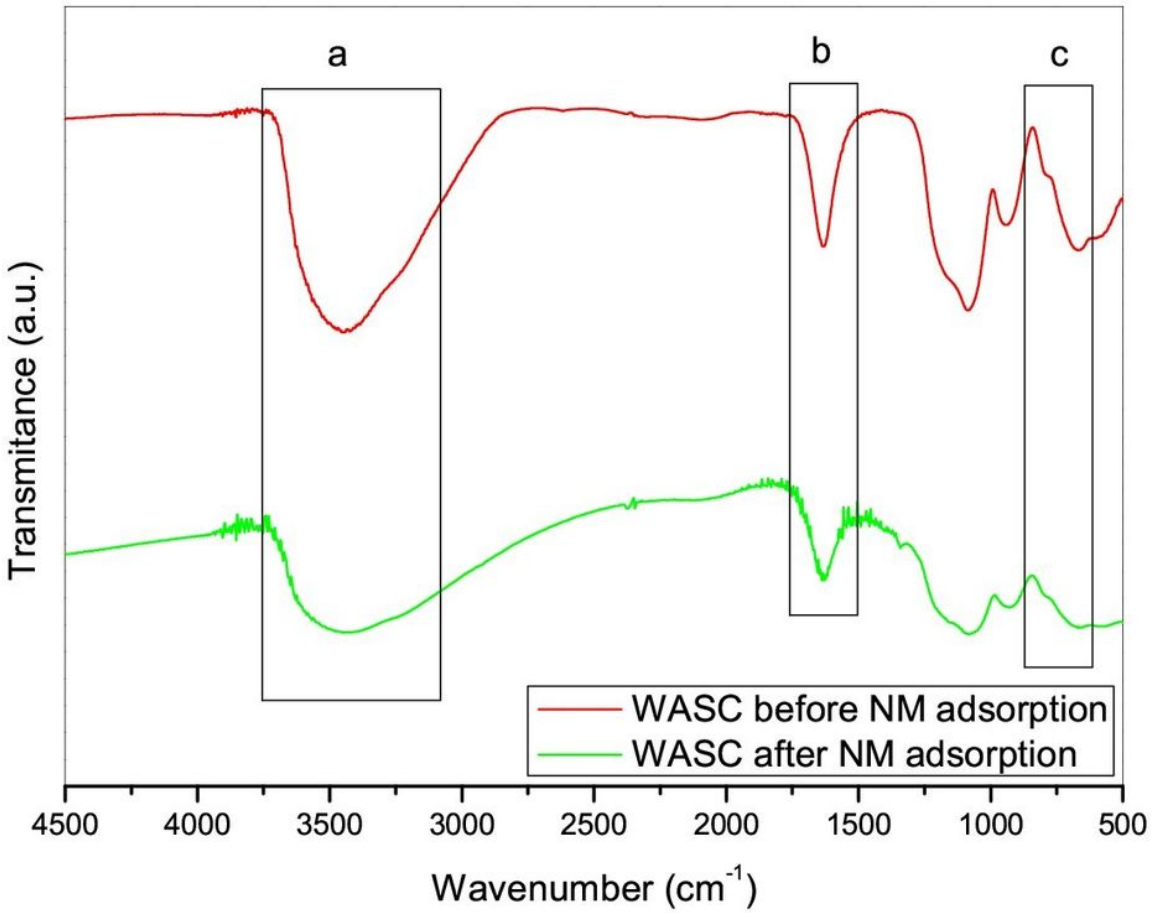

Figure 6

FT-IR spectra for WASC before and after the NM adsorption

Supplementary Files

This is a list of supplementary files associated with this preprint. Click to download.

- Table1.docx
- Table2.docx
- Table3.docx
- Table4.docx
- Table5.docx
- Table6.docx